Transactions of the 17th International Conference on Structural Mechanics in Reactor Technology (SMiRT 17)
Prague, Czech Republic, August 17 –22, 2003

Paper # F05-5

Creep Fracture and Creep Crack Growth in Inconel 718 Nickel based Superalloy

Antonietta Lo Conte

Politecnico di Milano, Department of Mechanical Engineering, Milan, Italy

ABSTRACT

The purpose of this investigation is to explore the creep rupture behaviour and creep crack growth of hot worked by forging Inconel 718 nickel based superalloy. Included in this study are the general crack growth characteristic and the relationship between the properties of smooth and notched specimen.

In order to investigate the creep deformation process, and the factor controlling the creep and the fracture behaviour, creep test has been carried out at 687 °C on specimen having longitudinal and transversal orientation with the temperature controlled to ±1 °C and at various constant loads below and close the material yield stress. Moreover creep crack growth test have been performed at the same temperature on ½ inch compact tension specimen having transversal orientation.

The comparison of the creep tests and creep crack growth tests allow us to observe that the sample orientation is a quite important factor influencing the crack behaviour.

KEYWORDS: Creep, Creep Crack Growth, Inconel 718

INTRODUCTION

The nickel based superalloy are a widely used group of materials for remarkable properties at elevated temperature and alloy IN718 represents almost half of the total tonnage of superalloy used worldwide [1],[2]. Creep crack growth is a major consideration in estimating the remaining life of elevated temperature components [3], [4], [5]. The presence of flaws due to manufacturing process of components and/or the corrosive environment, can be the cause of crack initiation and growth. It is important to predict either the incubation time and the creep crack growth rate for the reliability assessment of high temperature structural components.

The purpose of this investigation is to study the creep-rupture behavior and creep crack growth of hot worked by forging IN718 nickel based superalloy. Included in this study are the general crack growth characteristics and the relationship between the properties of smooth and notched specimens.

In order to investigate the creep deformation processes, and the factors controlling the tertiary creep and the fracture behaviour, creep tests and creep crack growth tests were carried out. The results allow us to observe that the sample orientation is a quite important factor influencing the crack behaviour.

Moreover the results of creep crack growth tests allows us to discuss the validity of fracture mechanics parameters for studying crack growth and interpret crack tip local damage in this alloy. Several models of creep crack growth have been discussed in literature. On the basis of the obtained results attempt will be made to assess, on the basis of the Nikbin, Smith and Webster approach [6], the time of crack initiation and the rate of damage accumulation.

EXPERIMENTAL PROCEDURE

The material used in this study was a commercial prepared Inconel 718 nickel superalloy, hot worked by forging in a 150 mm diameter bar, and having material composition listed in Table l. The heat treatment consisted of two hours at 1025 °C followed by water quenching, then six hours at 780°C followed by air cooling.

C	Si	Mn	P	S	Cr	Mo	Ni	Al	B	Co	Cu	Nb	Ti	Se	Ta	Fe	Pb	Bi
0.032	0.16	0.1	0.006	0.001	17.26	2.98	50.86	0.55	0.003	0.08	0.03	5.15	1.03	1ppm	0.007	bal.	1ppm	3ppm

Table 1 Chemical Composition of IN718.

Creep specimens were machined from the heat-treated bar, along its longitudinal and radial direction. The specimens had a 5 mm gauge diameter and a gauge length of 25 mm.

Creep tests were carried out in a Satec System constant load creep machines with a lever arm ratio of 20:1. Uniaxial tension creep experiments were performed in air at the temperature of t 687 °C and at the initial applied stress levels ranging from 350 to 650 MPa. The temperature of the sample was controlled by means of three thermocouples on the gauge length to ±0.5 °C of the set point. Creep strain measurements were obtained using an LVDT extensometer attached to the end sections of the specimen gauge length.

The specimen used for crack growth tests was the standard compact tension (CT) specimen configuration is shown in figure 1. The crack plane was parallel to the hot working direction and the crack grew in the radial direction. The CT specimens were fatigue pre-cracked, at room temperature, under constant amplitude loading, R=0.05, with maximum load equal 6.5 kN. The fatigue pre-cracks were grown between 2 and 4 mm from the notch root. Three samples were tested at 687 °C on the same Satec system used for creep tests. During the tests crack growth measurements were made by the electrical potential technique. A current of 10 A was used. The output voltage was converted to crack length using an experimental calibration curve previously developed by the author. After crack growth testing, the CT specimen was fractured and then the final crack length was measured. When the actual final crack length was different from the measured on by the potential method, the measured crack length was adjusted. Also, the crack opening displacements at the load line (pin centre to centre) were measured with two linear variable displacement transducers (LVDTs) .

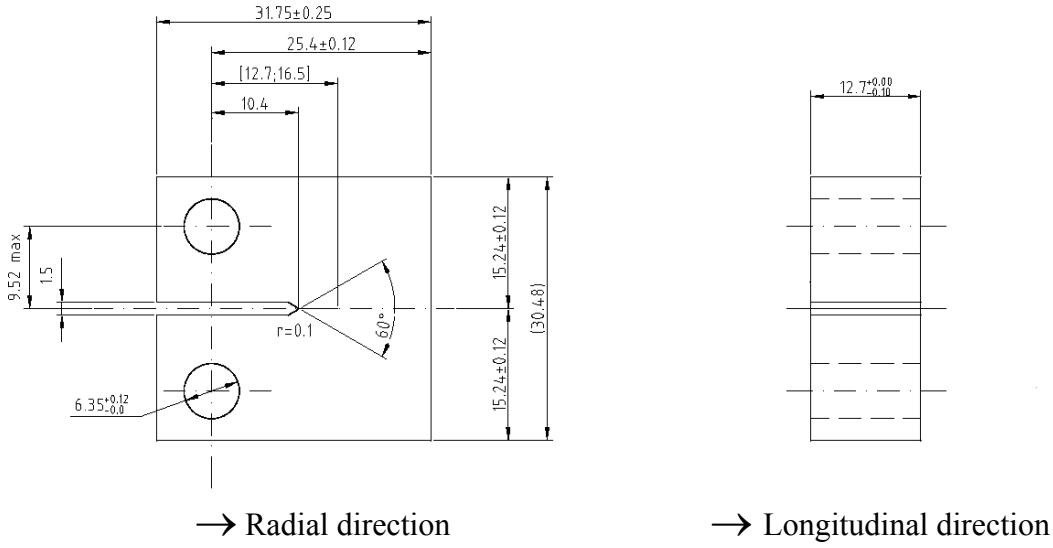

Figure 1 Compact Tension (CT) specimen configuration used for crack growth testing, dimension in mm.

RESULTS OF CREEP TESTS

Creep curve for tests performed in the longitudinal and transverse direction at 687 °C, at 560 MPa, are presented in figure 2. I It is clear from these figures that the creep response differs for the two orientations and that the creep resistance in the longitudinal orientation exceeds that in the transverse orientation. The primary transient creep of the longitudinal and transversal samples was of the normal type. But it is followed by a relatively short period of secondary creep, with creep rate in the transversal direction greater than the creep rate in the longitudinal direction, and by a period of accelerating creep rate, still greater in the longitudinal direction than in transversal, accounts for much of the life to rupture. This was found to be the case for all the stress levels investigated.

Figure 3 shows creep data for longitudinal and transverse direction plotted as strain rate and rupture life versus stress on double logarithmic axes.

The slopes of figure 3 correspond to the apparent stress exponents, for the longitudinal and transverse direction at the examined temperature and stress range, of the uniaxial creep law

$$\frac{\dot{\varepsilon}}{\dot{\varepsilon}_0} = \left(\frac{\sigma}{\sigma_0} \right)^n \qquad (1)$$

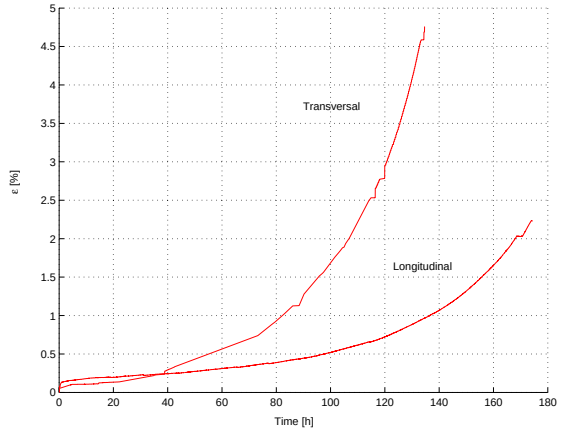

Figure 2 Creep curve for tests performed at 687 °C and 560 MPa.

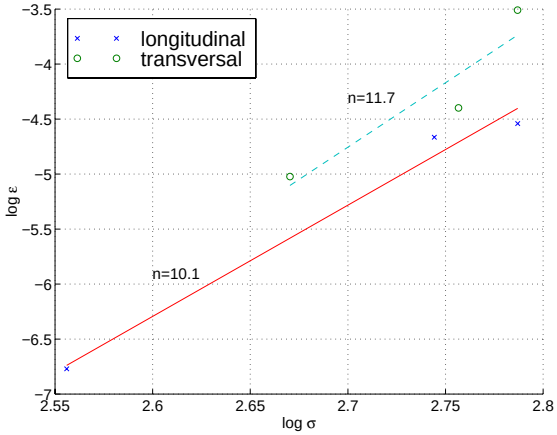

Figure 3 Strain rate versus stress on double logarithmic axes.

The apparent stress exponents results equal 10.1 in the longitudinal direction and equal 11.7 in the transversal direction. The observed shape o f creep curves are compatible with a dislocation substructure that is unstable to deformation, as postulated by other author [7].

Moreover another significant feature of the examined material is that the creep ductility is a critical parameter influencing the rate at which the tertiary creep develops and the failure occurs. Considering a typical creep curve as plotted in figure 1, an average creep strain $\dot{\varepsilon}_A$ can be defined in terms of the failure strain ε_f and rupture life t_R as

$$\dot{\varepsilon}_A = \frac{\varepsilon_f}{t_R} \tag{2}$$

which enables (1) to be written as

$$\dot{\varepsilon}_A = \dot{\varepsilon}_0 \left(\frac{\sigma}{\sigma_0} \right)^n \tag{3}$$

where the constants are now obtained from the rupture data rather than secondary creep properties as shown in figure 4. In addition for the stress rupture plot shown in figure 5

$$t_R = \frac{\varepsilon_{f0}}{\dot{\varepsilon}_0} \left(\frac{\sigma_0}{\sigma} \right)^\nu \tag{4}$$

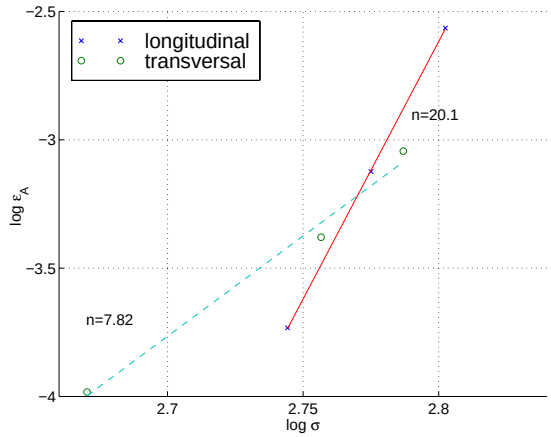

Figure 4 Average creep strain versus stress.

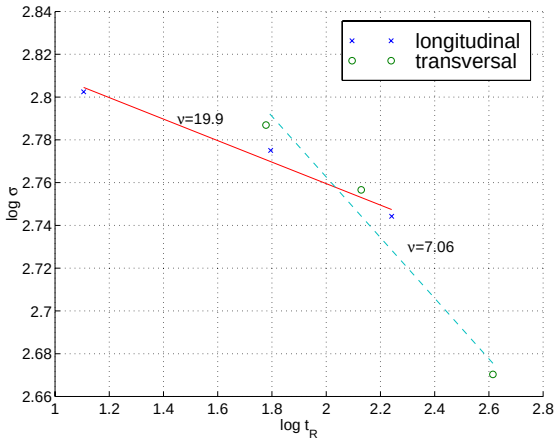

Figure 5 Stress versus rupture life.

giving

$$\varepsilon_f = \varepsilon_{f0}\left(\frac{\sigma}{\sigma_0}\right)^{n-\nu} \tag{5}$$

where ε_{f0} is the uniaxial creep failure strain at stress σ_0. For $n > \nu$ .the ductility decreases with decrease in stress.

As results from the figure 4 and 5 the decreasing of the material ductility a failure in creep with decrease in stress occurs both for longitudinal and transversal direction, but the reduction is more evident in transversal direction than in the longitudinal one.

According the Nikbin, Smith and Webster damage accumulation model, these features will be used in the next paragraph, joint with a creep crack growth models, in order to predict the crack propagation rate in the present nickel based superalloy.

RESULTS OF CREEP CRACK GROWTH TESTS

Fracture surface of the Compact Tension sample tested with K_I equal to 22 MPa $m^{1/2}$ is shown in figure 6 where the extension of the fatigue propagation, the extension of the creep crack growth and the final brittle rupture, are also indicated. The relationship of crack length versus time at 687 °C obtained in this tests are shown in figure 7, for three different initial values of K_I. The test carried out with K_I equal 22 MPa $m^{1/2}$ has been interrupted after 116 hours.

The value of crack initiation can be defined as corresponding to Δa = 0.2 mm [8] and the initiation time can be obtained directly by the potential drop measurement as reported in table 2. For the non interrupted tests, it can be observed that the initial transition crack growth stage occupied about 20 % of life, the constant crack growth rate period occupied about 50% of life and accelerating crack growth occupied about 30% of life. Hence, the constant rate period occupied a large part and the accelerating period occupied a small part of the rupture life. The increase of creep crack during the constant rate period was small and crack grew rapidly during the acceleration stage. The values of creep crack extension rate during the stationary are reported in table 2.

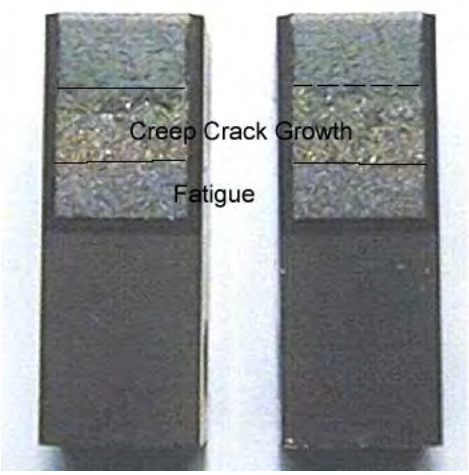

Figure 6 Fracture surface of the Compact Tension sample tested with K_I equal to 22 MPa $m^{1/2}$.

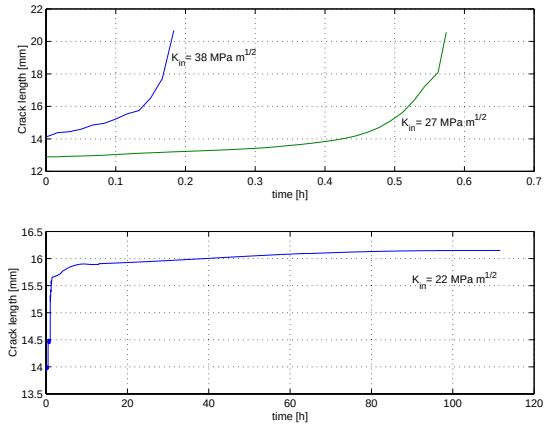

Figure 7 Creep crack length versus time for three different initial values of K_I.

K_I	[MPa $m^{1/2}$].	22	27	38
t_i	[h]	5.7	0.12	0.02
da/dt	[mm/h]	1.05 10^{-3}	1.67	11.91

Table 2 Initiation time and stationary creep crack extension rate.

Figure 8 shows the relationship of crack length versus time at 687 °C obtained for the three examined initial values of K_I. After the displacement due to the load application, a primary creep type behaviour prevail during same portion of the initiation time, manifesting in the form of decreasing displacement rate with time. The crack tip opening displacement at initiation time can be obtained from load line displacement and is reported in Table 3.

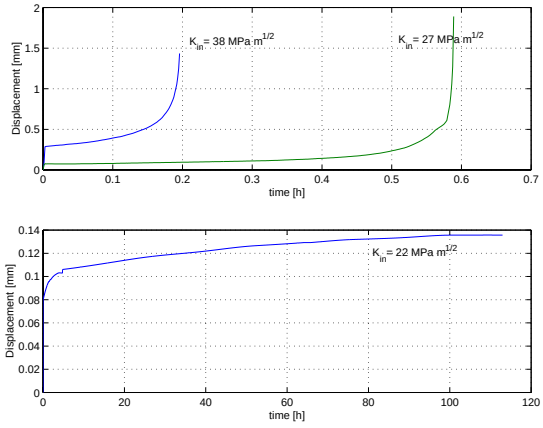

Figure 8 Load line displacement versus time for three different initial values of K_I.

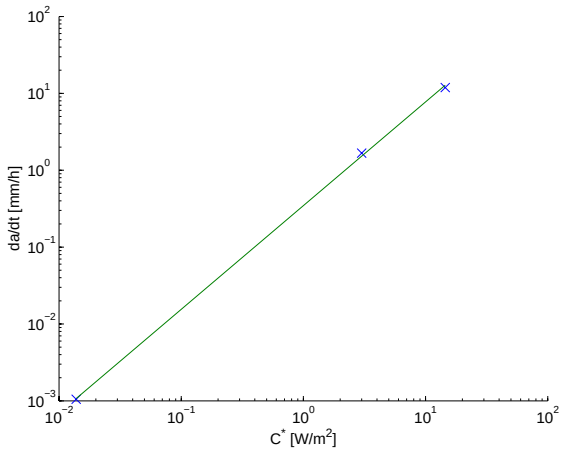

Figure 9 The creep crack growth extension rate versus C*.

K_I [MPa m$^{1/2}$].	22	27	38
$CTOD_i$ [mm]	0.099	0.048	0.002
C^* [W/m^2]	1.38 10^{-2}	3.0	14.5

Table 3 CTOD at initiation time and integral C^*.

For extension following initiation, it is usual relate creep crack extension rate $\dot{\Delta}_c$ to a fracture mechanics parameter C*. For tests carried out with constant applied load F, the C* parameter is determined using the expression provided in ASTM E1475

$$C^*(t) = \eta \frac{F\dot{\Delta}_c}{B \cdot (W-a)} \frac{n}{n+1} \qquad (6)$$

where

W is the specimen width
B is the net specimen section
η is determined for the initial crack length
n is the stress index in power law creep for transversal direction

The values of the fracture mechanics parameter C^* during the stationary period are reported in table 3 and the plot of crack growth extension rate versus C^* is reported in figure 9.

For material in which secondary creep dominates, and the axial creep low can be written as (1) the stress field at coordinates (r, θ)

$$\frac{\sigma_{ij}}{\sigma_0} = \left(\frac{C^*}{I_n \sigma_0 \dot{\varepsilon}_0 r} \right)^{\frac{1}{n+1}} \overline{\sigma}_{ij}(\theta, n) \qquad (7)$$

where σ_{ij} is the stress tensor and $\overline{\sigma}_{ij}(\theta, n)$ is a non-dimensional function of n and θ chosen so that the effective stress has a maximum magnitude of 1. The factor I_n is postulated as a function of n, but for most value of n of practical interest, and for plane stress conditions, it can be expressed approximately as 3.

The equation (7) indicates that, when $n=1$, C^* predicts the same stress distribution ahead a crack as K. In the limit $n \to \infty$ the singularity at the crack tip disappears, in this condition C^* and the net section stress give the same results.

The experimentally evaluated values of C^* can be incorporated, jointly with the uniaxial power law exponent in the transversal direction, into the Nikbin, Smith and Webster crack growth model able to predict crack propagation in a range of alloys having a wide spread of creep properties and ductilities.

The NSW model supposes that ahead of a growing crack there is a process zone, with characteristic dimension r_c. As cracking proceeds damage will first be experienced by an element of material when it is enters the creep zone at r =r_c and it is assumed that local fracture will occur at the crack tip when the creep ductility of the material is exhausted here.

When secondary creep dominates and creep failure strain is constant it has been shown that the equation (7) can be inserted into the NSW model to give an expression for creep crack growth rate as

$$\dot{a} = (n+1)\frac{\dot{\varepsilon}_0}{\varepsilon^*_f}\left(\frac{C^*}{I_p \sigma_0 \dot{\varepsilon}_0}\right)^{n/(n+1)} r_c^{(1)/(n+1)} \qquad (8)$$

where ε^*_f is the creep ductility appropriate to the state of stress local to the crack tip.

Substitution of (5) and (3) into the NSW damage accumulation model results in a modified crack growth rate expression

$$\dot{a} = \left(\frac{n+1}{n+1-\upsilon}\right)\frac{\dot{\varepsilon}_0}{\varepsilon^*_{f0}}\left(\frac{C^*}{I_p \sigma_0 \dot{\varepsilon}_0}\right)^{\upsilon/(n+1)} r_c^{(n+1-\upsilon)/(n+1)} \qquad (9)$$

If in this correlation, the size of the process zone is assumed to be the material grain size, the creep ductility at the crack tip taken to be 1/50 of the uniaxial creep ductility , n and ν are obtained from the figure 4 and 5, then the values reported in table 4, for the creep crack extension rate, are obtained.

The comparison of the calculated values with the experimental ones allows us to observe that the NSW model give an acceptable prediction of the creep crack growth rate from the knowledge of the creep failure strain. Moreover, the calculated values have been obtained using for each level of K_I the same size of the encompassed zone. The results would be in better accordance with the measured ones if a more confident value of this parameter were known.

At the end it will be observed that the fracture parameter C* cannot uniquely characterises the creep crack growth in Nickel superalloy and, as observed by some authors [9], its use is partially limited.

C^* [W/m^2]	1.38 10^{-2}	3.0	14.5
da/dt [mm/h]	4.49 10^{-3}	0.32	1.17

Table 4 Calculated creep crack growth rate.

CONCLUSION

The comparison of the creep tests and creep crack growth tests allow us to observe that the sample orientation is a quite important factor influencing the crack behaviour.

The adoption of uniaxial creep parameters, measured with creep tests, has enabled to predict the creep crack growth rate, by means of NSW damage model, that shows a good accordance with the measured creep crack growth in the experimental tests.

REFERENCES

1. Jianting G., Ranucci D., Picco E. and Strocchi P.M., "An Investigation on the Creep and Fracture Behavior of Cast Nickel-Base superalloy IN738LC", *Metallurgical Transactions A*, Vol.14A, 1983, pp. 2329-2335.
2. Tian S.G., Zhang J. H., Zhou H. H., Yang H. C., Xu Y. B. and Hu Z. Q., "Creep Behaviour of Single Cristal Nickel Base Superalloy", *Material Science and Technology*, Vol. 14, 1998, pp. 751-756.
3. Floreen S., "The Creep Fracture of Wrought Nickel-Base Alloys by a Fracture Mechanics Approach"*, Metallurgical Transactions A*, Vol.6A, 1975, pp. 1741-174.
4. Andersson H., Perrson C.,and Hansson T. "Crack Growth in IN718 at High Temperature*", Internationl Journal of Fatigue.*, Vol. 23, 2001, pp. 817-827.
5. Wanhill R.J.H., "Significance of Dwell Cracking for IN718 Turbine Discs", *Internationl Journal of Fatigue*, Vol.24, 2002, pp. 545-555.
6. K. M. Nikbin, D. J. Smith, G. A. Webster, An Engineering Approach to the Prediction of Creep Crack Growth, Journal of Engineering Materials and Technology, Vol. 108, April 1986, pp. 186-191.
7. Dyson B. F. and Gibbons T. B., "Tertiary Creep in Nickel-Base Superalloys: Analysis of Experimental Data and Theoretical Sinthesys", *Acta metallurgica*, Vol.35, No. 9, 1987, pp. 2355-2369.
8. Schwalbe K. H., Ainsworth R. A., Saxena A. and Yokobory T., "Reccomendation for a Modification of ASTM E1457 to Include Creep-Brittle Materials", *Engineering Fracture Mechanics*, Vol. 62, 1999, pp. 123-142.
9. Tabuchi M., Kubo K., Yagi K., Yokoboki A. T. and Fuji A., "Results of a Japanese Round Robin on Creep Crak Growth Evaluation Methods for Ni-Base Superalloys", *Engineering Fracture Mechanics*, Vol. 62, 1999, pp. 47-60.
10. Tong J., Dalby S., Byrne J., Henderson M.B. and Hardy M.C., "Creep, Fatigue and Oxidation in Crack Growth in Advanced Nickel Base Superalloys", *Internationl Journal of Fatigue.*, Vol. 23, 2001, pp. 897-902.